

---

# Trustworthy Machine Learning for Interpretable Early Warning of Diabetes: Modern Ensembles and Tabular Deep Learning with Causal Inference, Counterfactuals, and Uncertainty

---

[Kazi Sakib Hasan](#) \*

Posted Date: 7 May 2025

doi: 10.20944/preprints202505.0292.v1

Keywords: Causal Inference; Trustworthy ML; Tabular Deep Learning; Diabetes Early Warning



Preprints.org is a free multidisciplinary platform providing preprint service that is dedicated to making early versions of research outputs permanently available and citable. Preprints posted at Preprints.org appear in Web of Science, Crossref, Google Scholar, Scilit, Europe PMC.

Copyright: This open access article is published under a Creative Commons CC BY 4.0 license, which permit the free download, distribution, and reuse, provided that the author and preprint are cited in any reuse.

Article

# Trustworthy Machine Learning for Interpretable Early Warning of Diabetes: Modern Ensembles and Tabular Deep Learning with Causal Inference, Counterfactuals, and Uncertainty

Kazi Sakib Hasan

Department of CSE, BRAC University, Kha 224, Bir Uttam Rafiqul Islam Ave, Dhaka, 1212, Bangladesh;  
kazi.sakib.hasan@g.bracu.ac.bd

**Abstract:** Globally, an estimated 589 million adults (20-79 years) are living with diabetes, with 1 in 9 individuals affected. Beyond traditional diagnostic and early detection systems, machine learning is already implemented to diagnose the disease. Nevertheless, there are several gaps that are not addressed so far. In this research, a trustworthy machine learning framework is proposed for early warning of diabetes that integrates causal inference, interpretability, modern ensemble methods, and tabular deep learning to address the critical demands of reliability, fairness, and interpretability in clinical AI systems. The study utilizes a diverse model suite including LightGBM, XGBoost-DART, HistGBM, and TabNet, along with a novel Causal-guided Stacking Classifier (CGSC) using LightGBM as the meta-learner. Causal Forests are employed for feature selection to prioritize stable and causally-relevant predictors in this particular model. For interpretability, SHAP is leveraged to provide global, local, and mean feature attribution for the best-performing ensemble, while TabNet's built-in attention mechanism is used to highlight local explanations and feature salience. As a basic fairness-aware design choice, gender was excluded as a feature to examine bias mitigation without compromising performance. Uncertainty quantification of the ensemble models is also provided. Counterfactuals are added for personalized disease prevention attempts. Our results indicate that the CGSC achieved the highest recall (0.81) with minimal F1-score uncertainty ( $0.73 \pm 0.03$ ), demonstrating strong predictive reliability. All experiments are fully reproducible, with resources available at the GitHub repository.

**Keywords:** causal inference; trustworthy ML; tabular deep learning; diabetes early warning

## 1. Introduction

Diabetes mellitus represents one of the most significant global health challenges of the 21st century with escalating incidence and economic burden. As of 2021, 537 million adults were living with diabetes approximately, a number projected to rise to 643 million by 2030 and 783 million by 2045 [1]. Recent updates suggest that approximately 1 in 9 adults globally now live with the condition that indicates a widening health crisis which disproportionately affects low- and middle-income countries [2]. Diabetes contributes significantly to healthcare expenditure beyond individual morbidity, with global costs exceeding USD 966 billion annually [3]. Early warning and timely detection of diabetes is critical. Because delayed diagnosis can lead to severe long-term complications including neuropathy, cardiovascular disease, retinopathy, and kidney failure [4]. However, early-stage diabetes often presents with nonspecific or asymptomatic clinical signs that makes it challenging to identify without proactive screening tools [5]. Now, most of the current screening systems are based on threshold criteria, such as fasting plasma glucose, oral glucose tolerance test (OGTT), or HbA1c levels [7]. These biomarkers are clinically validated, but are limited by their binary nature which makes them fail to capture the nuanced continuum of glucose dysregulation [8]. Additionally, factors like biological variability, stress, medication, and ethnicity can influence these metrics that can potentially

lead to false positives or missed diagnoses [9]. Moreover, traditional methods rarely account for the interplay of multiple risk factors like as BMI, blood pressure, lipid profiles, and family history within a holistic framework, and it cannot warn the individuals early. If early detection or warning is provided with counterfactuals, individuals can follow preventive measures against diabetes. The siloed approach of traditional diagnosis restricts the ability to detect early pathophysiological changes or tailor interventions based on individual profiles [10]. Screening tools like the Finnish Diabetes Risk Score (FINDRISC) offer some multivariable prediction but their predictive power remains modest across diverse populations [11]. The lack of adaptability and personalization in these systems underscores the pressing need for more dynamic, data-driven solutions that can learn from complex patterns across diverse populations.

The global expansion of digital health records, biometric data, and health-related behavioral tracking offers new opportunities to enhance disease detection. In this data-rich context, machine learning (ML) has emerged as a promising avenue to uncover hidden patterns and predictive markers in large-scale tabular data [6]. The increasing digitization of healthcare, generally due to the widespread availability of electronic health records (EHRs) and biometric data, has opened a path for machine learning (ML) to play a transformative role in disease diagnosis, and so do in risk stratification. In the context of diabetes, ML models provide distinct advantages over traditional diagnostic systems by enabling the discovery of complex and nonlinear relationships among numerous clinical and behavioral variables. Algorithms like decision trees, support vector machines, and ensemble methods such as random forests have demonstrated improved accuracy in identifying undiagnosed diabetes or predicting future onset compared to conventional models [12]. These predictive techniques are particularly well-suited for tabular medical data that allows for the inclusion of a wide array of risk factors such as age, BMI, blood pressure, lipid profiles, and lifestyle indicators without the need for pre-specified interactions [13]. Furthermore, ML frameworks can be continuously updated as new data becomes available. Thus, it supports dynamic learning and adaptation to evolving population health trends. Nevertheless, even after having all these advantages, widespread clinical adoption of ML remains constrained by critical challenges in interpretability, fairness, and reliability that are essential in healthcare contexts where transparency and trust are necessary for clinical decision-making. A big step toward enabling more ethical, scalable, and personalized early detection systems is to address these issues.

Machine learning systems are increasingly integrated into clinical workflows, and hence the demand for trustworthy AI systems that are not only accurate but also reliable, fair, and interpretable is growing significantly. In healthcare, the stakes are particularly high because predictions directly impact patient outcomes, influence clinical decisions, and affect resource allocation. Trustworthiness in this domain encompasses several critical dimensions that includes but may not be limited into robustness to data shifts, transparency of model decisions, mitigation of bias, and accountability for outcomes [16]. A foundational role in ensuring trust is played by interpretability as well. Clinicians must be able to understand why a model arrives at a particular prediction, mainly when it contradicts clinical intuition. Black-box models, even when accurate, are often met with resistance in healthcare due to the lack of explanatory power [17]. Moreover, fairness and bias mitigation are essential, as healthcare datasets often reflect underlying social inequities. If these biases are unchecked, they can propagate through algorithms, and later will disproportionately affect the vulnerable populations. As regulatory frameworks such as the European Union's AI Act and U.S. FDA guidelines evolve, healthcare ML systems will increasingly need to demonstrate transparency, equity, and robustness in real-world deployment. The development of trustworthy AI systems is thus not solely a technical challenge but a multidimensional task that intersects with ethics, policy, and clinical practice.

Furthermore, despite advances in machine learning for diabetes detection, most existing studies continue to focus narrowly on predictive accuracy, and leave several critical dimensions unaddressed. Many models rely on correlational features derived from statistical associations, which may not generalize across populations or offer clinically meaningful insights. Without a causal grounding,

such models are limited in their ability to support reasoning about interventions or explain why a particular prediction occurs. Moreover, interpretability remains underdeveloped in ensemble and deep models. These architectures excel at capturing complex patterns, but they often obscure the decision process, and make it difficult for clinicians to trust or act upon individual predictions. Even when interpretability tools are used, they rarely connect insights to potential interventions. Another major shortfall is the limited use of counterfactual reasoning. Existing ML systems almost never explore what-if scenarios to suggest preventive pathways or minimal changes needed to reduce risk. This absence restricts their role from passive prediction to active clinical decision support. Adding to these, fairness is also often sidelined. Many studies fail to examine model behavior across demographic subgroups or mitigate bias in feature selection and outcome prediction. Ultimately, few frameworks holistically integrate causality, interpretability, fairness, and actionable counterfactuals, that leave a significant gap in the development of clinically trustworthy AI systems.

Therefore, the above-mentioned gaps are tried to cover in this research. The major contributions of the research are outlined below:

- Proposed a novel **Causal-guided Stacking Classifier (CGSC)** that integrates causal feature selection, ensemble learning, and interpretability to enhance trustworthiness in early diabetes detection.
- Employed **Causal Forests** for feature selection to identify stable, causally-relevant predictors, ensuring robustness against data shifts and improving generalizability.
- Experimentally applied a newborn and underutilized modern tabular deep learning model named TabNet.
- Designed and implemented **counterfactual reasoning mechanisms** to suggest preventive and actionable feature-level interventions for high-risk individuals.
- Conducted **uncertainty analysis** using F1-score distribution metrics to evaluate model reliability and prediction stability across multiple training iterations.
- Applied **SHAP-based feature attribution** for global and local interpretability, and leveraged TabNet's attention mechanism to visualize feature salience for individual predictions.

## 2. Literature Review

Ghosh and Argal (2024) proposed a robust ensemble learning framework by integrating exploratory data analysis (EDA) with multiple classifiers that includes Random Forest, Gradient Boosting, and XGBoost. They attempted to predict the onset of diabetes. Their approach began with data pre-processing and correlation mapping to uncover hidden variables affecting diabetes prediction. The ensemble models outperformed traditional single classifiers with the highest accuracy reaching 89.6% on the Pima Indian Diabetes dataset. The study highlights the synergistic impact of pre-modeling insights and ensemble learning in medical diagnostics. Furthermore, it emphasizes interpretability through SHAP values and feature importance rankings, to ensure transparency in model predictions [18].

Kirubakaran et al. (2025) introduced a fuzzy support vector regression (FSVR) model tailored for progressive diabetes detection. The study aimed to mitigate the high false-positive rate prevalent in binary classifiers by incorporating fuzzy logic to handle uncertainty in patient data. The model achieved 91.2% accuracy and displayed strong resilience against noisy features on real-world clinical dataset. Unlike black-box models, FSVR offered interpretable decision boundaries. This feature makes it a preferred choice in clinical settings requiring transparency. The authors recommend expanding this framework with hybrid optimization methods for future scalability [19].

Alkhaldi et al. (2025) explored the use of biochemical markers such as liver enzymes (ALT, AST) and BMI for early type 2 diabetes detection through gradient boosting machines and logistic regression. Their retrospective study utilized a public dataset of over 5,000 patients, and obtained an AUC-ROC of 0.93. Notably, the model identified ALT as a stronger predictor than BMI, that challenges traditional clinical assumptions. The researchers also integrated SHAP for feature attribution and confirmed

that their model maintained high sensitivity across diverse demographic subgroups. This research illustrates the practicality of non-invasive, low-cost diagnostics supported by machine learning [20].

Meng et al. (2025) presented a breakthrough in non-invasive diagnosis of diabetic kidney disease (DKD) using deep learning models applied to retinal fundus images. The model successfully differentiated DKD from isolated diabetic nephropathy with an AUC exceeding 0.95 by training convolutional neural networks (CNNs) on a large population-based dataset. This study leveraged retinal imaging as a proxy for renal pathology, significantly reducing the need for invasive biopsies. It introduced a novel diagnostic paradigm that aligns with precision medicine goals and facilitates earlier intervention. The research is notable for its translational potential and practical deployment in primary care settings [21].

Sushith et al. (2025) developed a hybrid deep learning framework combining convolutional neural networks (CNNs) and recurrent neural networks (RNNs) for early detection of diabetic retinopathy. The model utilized spatial features via CNNs and temporal progression cues via RNNs to monitor disease development. Evaluation on benchmark datasets revealed a superior performance over standalone CNNs, that attained 96.1% accuracy. The model also demonstrated high specificity which makes it valuable for screening applications. Their pipeline underscores the importance of modeling time-dependent patterns in chronic disease diagnostics using hybrid deep learning [22].

Xiao et al. (2025) introduced an interpretable machine learning model guided by biomarker relevance for diabetes diagnosis. The study emphasized transparent feature selection and interpretability utilizing logistic regression and decision trees, which is critical in healthcare. Using a Chinese cohort with biomarkers like HbA1c, insulin, and triglycerides, the model reached an 87% prediction accuracy. The authors incorporated SHAP values to highlight influential features, and their framework was validated through clinician interviews. This study bridges the gap between data-driven insights and clinical interpretability that enables the trustworthiness of AI in diagnostics [23].

Wang et al. (2025) developed a novel approach for classifying diabetic retinopathy using a Single Shot Multibox Detector (SSD)-based deep learning model. The architecture was trained on high-resolution retinal fundus images to detect disease stages ranging from mild to proliferative retinopathy. Compared to traditional CNN architectures, SSD enabled real-time lesion detection with over 93% accuracy and demonstrated high sensitivity in detecting early-stage indicators. This model's speed and accuracy make it highly suitable for deployment in low-resource clinical settings, where rapid screening is essential [24].

Gupta et al. (2025) proposed a Quantum Transfer Learning (QTL) method for enhancing diabetic retinopathy detection. Their model combined ResNet-based feature extraction with a quantum-enhanced classification layer, aiming to leverage quantum computing's parallelism. Tested on public ophthalmic datasets, the QTL model outperformed classical deep learning baselines in both precision and inference time. The hybrid model achieved a classification accuracy of 95.3%, and the study highlighted potential applications of quantum AI in medical imaging, setting the stage for faster and more energy-efficient diagnostics [25].

Ge et al. (2025) addressed the early prediction of low muscle mass (LMM) in patients with diabetes and obesity through supervised machine learning. Using clinical, metabolic, and demographic features, their random forest-based model yielded an AUC of 0.88 and emphasized body fat percentage, serum albumin, and HbA1c as key predictors. The model assists clinicians in identifying LMM risk—an often-overlooked comorbidity—in diabetic populations. It also offers actionable insights for early intervention strategies such as resistance training and nutritional therapy [26].

Most of the research in the literature focuses on diabetes diagnosis and interpretability. A little research is conducted on early warning systems for diabetes that require no clinical intervention. Such systems, if integrated with counterfactuals, have the ability to provide preventive measures against diabetes to the individuals. Also, feature selections are usually correlation-based, even though a causal inference-based feature selection could be more robust. Therefore, in this research, these gaps are tried to cover.

### 3. Methodology

This section describes the workflow of how the research is conducted. GitHub repository of this research contains every file and resource that are necessary to replicate this study in future. [27]

#### 3.1. Dataset Information

A dataset from Kaggle, entitled “diabetes\_data” uploaded by Prosper Chuks is utilized for modeling purposes. The dataset has 70692 instances, and 18 columns with 17 features and a target variable. The features contain internal and external physical attributes, lifestyle choices, and demographic information about each individual, whereas the target column contains whether the individual has diabetes or not. The dataset contains the following columns: Age, Sex, HighChol, CholCheck, BMI, Smoker, HeartDiseaseorAttack, PhysActivity, Fruits, Veggies, HvyAlcoholConsump, GenHlth, MentHlth, PhysHlth, DiffWalk, Stroke, HighBP, and Diabetes. Definitions of each column and the values they take are given in Table 1. It is noticeable that, knowing the information of these variables does not require any clinical intervention. Therefore, developing an early warning system for diabetes utilizing machine learning algorithm is possible with this dataset.

**Table 1.** Variable Definitions and Values for the Diabetes Diagnosis Dataset

Variable	Definition	Values
Age	Age category of the person	13-level categorical. 1 = 18–24; 9 = 60–64; 13 = 80+
Sex	Sex of the person	0 = Female; 1 = Male
HighChol	High cholesterol status	0 = No; 1 = Yes
CholCheck	Cholesterol check in last 5 years	0 = No; 1 = Yes
BMI	Body Mass Index	Continuous positive values
Smoker	Smoked at least 100 cigarettes in life-time	0 = No; 1 = Yes
Heart..Attack	Ever had heart disease or attack	0 = No; 1 = Yes
PhysActivity	Physical activity other than job	0 = No; 1 = Yes
Fruits	Consumes fruit at least once daily	0 = No; 1 = Yes
Veggies	Consumes vegetables at least once daily	0 = No; 1 = Yes
Hvy..Consump	Heavy alcohol consumption ( $\geq 14$ drinks/week for men, $\geq 7$ for women)	0 = No; 1 = Yes
GenHlth	General health status	Ordinal: 1 = Excellent to 5 = Poor
MentHlth	Poor mental health days per month	0 to 30 (ordinal)
PhysHealth	Poor physical health days per month	0 to 30 (ordinal)
DiffWalk	Difficulty walking or climbing stairs	0 = No; 1 = Yes
Stroke	Ever had a stroke	0 = No; 1 = Yes
HighBP	High blood pressure status	0 = No; 1 = Yes

#### 3.2. Data Preprocessing

The dataset has no null values or duplicate values. Moreover, the data has no non-numeric columns that require numeric encoding as well. However, the target variable was in float data type which is later transformed into integer in order to avoid complexities. To minimize the risk of demographic bias,, the “Sex” column is dropped. While this step removes direct influence and solves most of the problem, the model can still learn indirect bias (latent bias) unless explicitly tested for it. Delving deeper into such forms of bias mitigation require extensive analysis like testing for proxy bias, training with reweighting or adversarial debiasing, and fairness-aware modeling techniques that are beyond the scope of this research.

The dataset has heteroskedasticity issues as shown in Figure 1. Note that, the bar chart of standard deviation is shown instead of variance. Because some features have a larger range of values, and hence their variance takes far more upper range in the y-axis, which makes it unclear to look at the feature variances with lower magnitude.

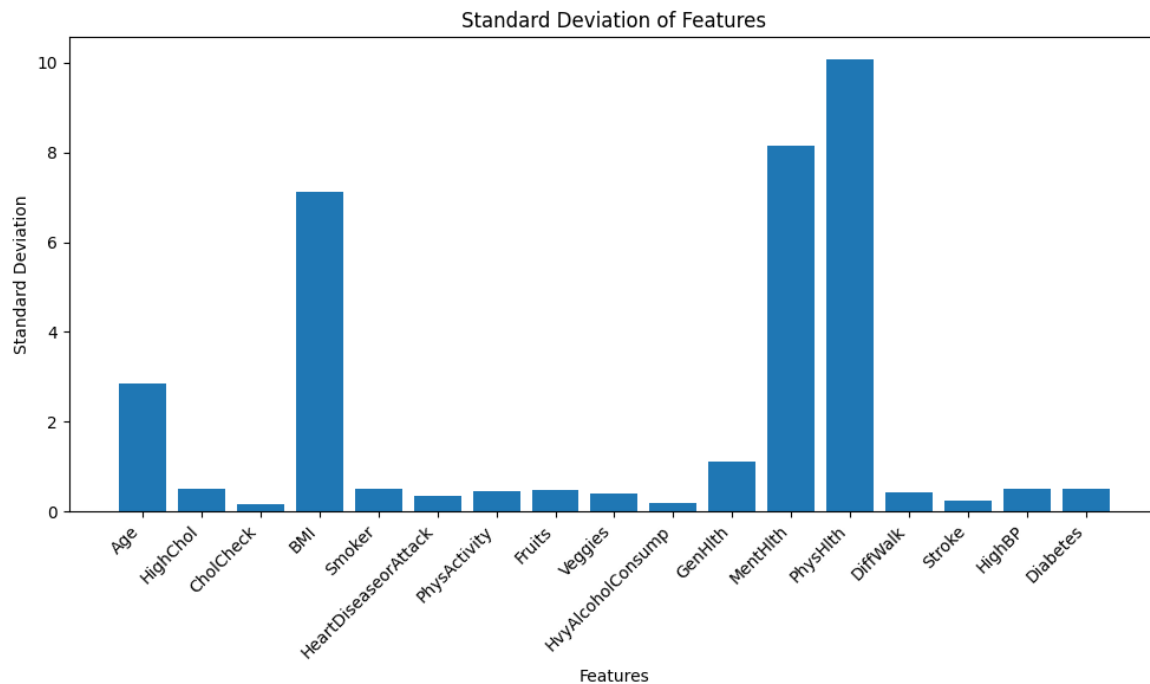


**Figure 1.** Heteroskedasticity Among the Features

For parametric models like Logistic Regression or Neural Networks, heteroskedasticity causes a problem by emphasizing more on the features having higher range of values. Conversely, for non-parametric models like NGBoost or any other ensemble models, it does not create any problem as these models learn internal data patterns with decision rules. Therefore, the data is not scaled at this stage. However, during the training of TabNet- which is a tabular neural network, the data was scaled using z-score standardization from scikit-learn's StandardScaler().

Figure 2 presents a visual comparison between diabetes and non-diabetes instances in the dataset based on their clustering behavior. To enable this, Principal Component Analysis (PCA) was employed to reduce the original high-dimensional feature space into two principal components. These two components capture the maximum variance in the data and serve as the new feature axes for visualization. The resulting 2D scatter plot distinctly shows how individuals with and without diabetes are distributed in the transformed space, thereby offering insights into potential separability of the classes using machine learning methods.

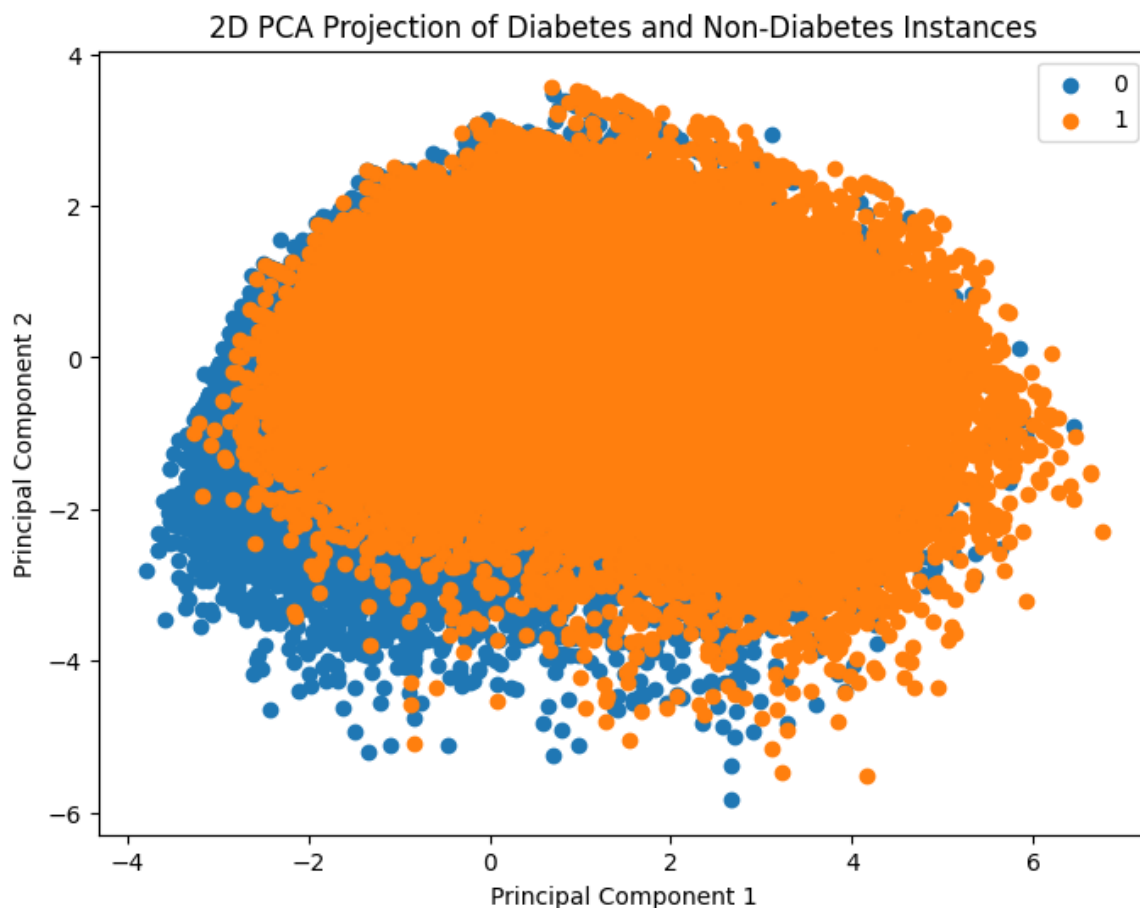


**Figure 2.** Principal Component Analysis (PCA) Visualization Showing Class-Wise Distribution of Diabetes and Non-Diabetes Instances

A correlation heatmap of the features is shown in Figure 3. It is shown that several low to moderate correlations between the features exist. For example, "GenHlth" and "PhysHlth" are moderately correlated with a coefficient of 0.55. Worsening of "GenHlth" is also slightly associated with heart diseases or attack with a correlation coefficient of 0.28.

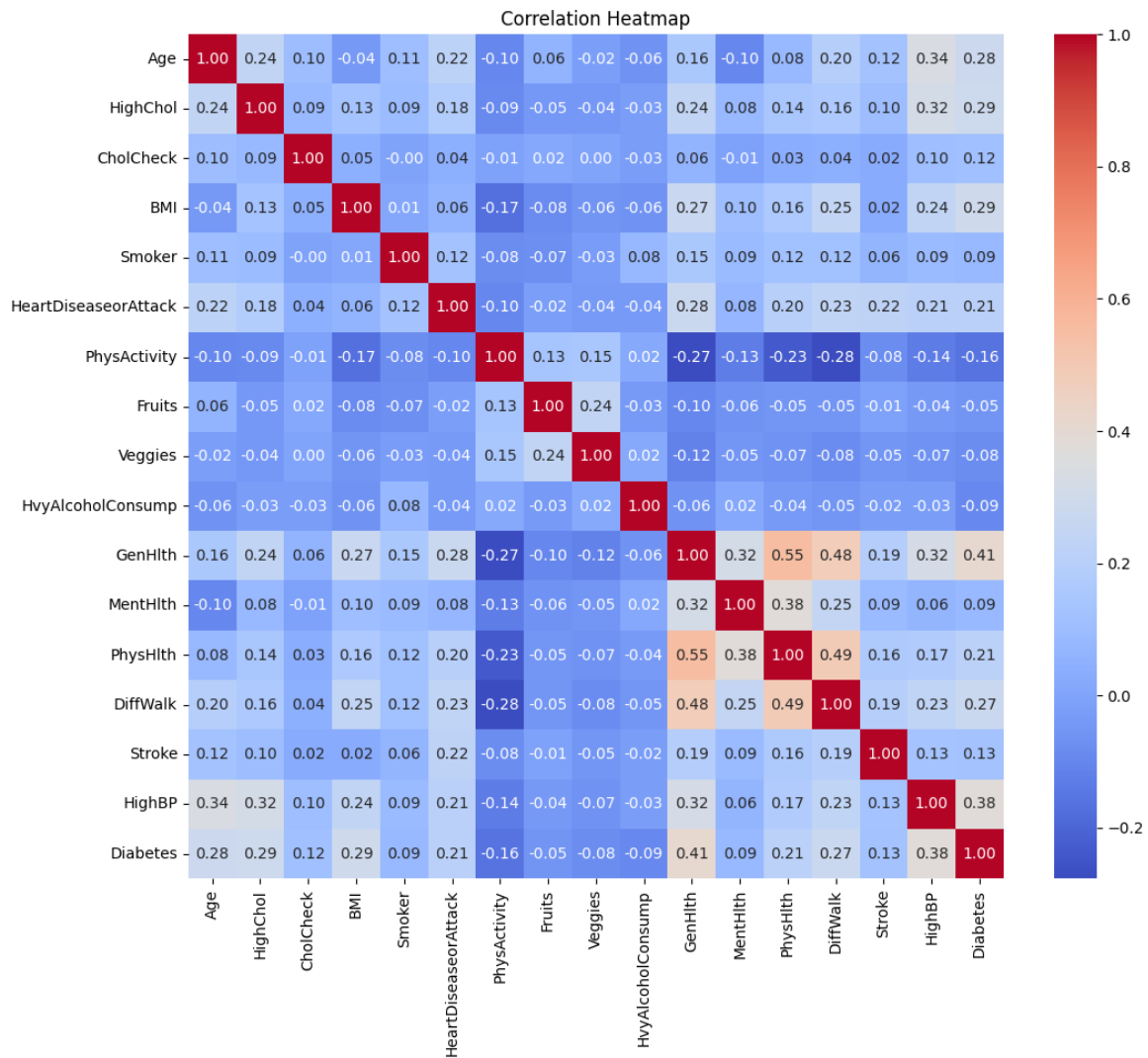
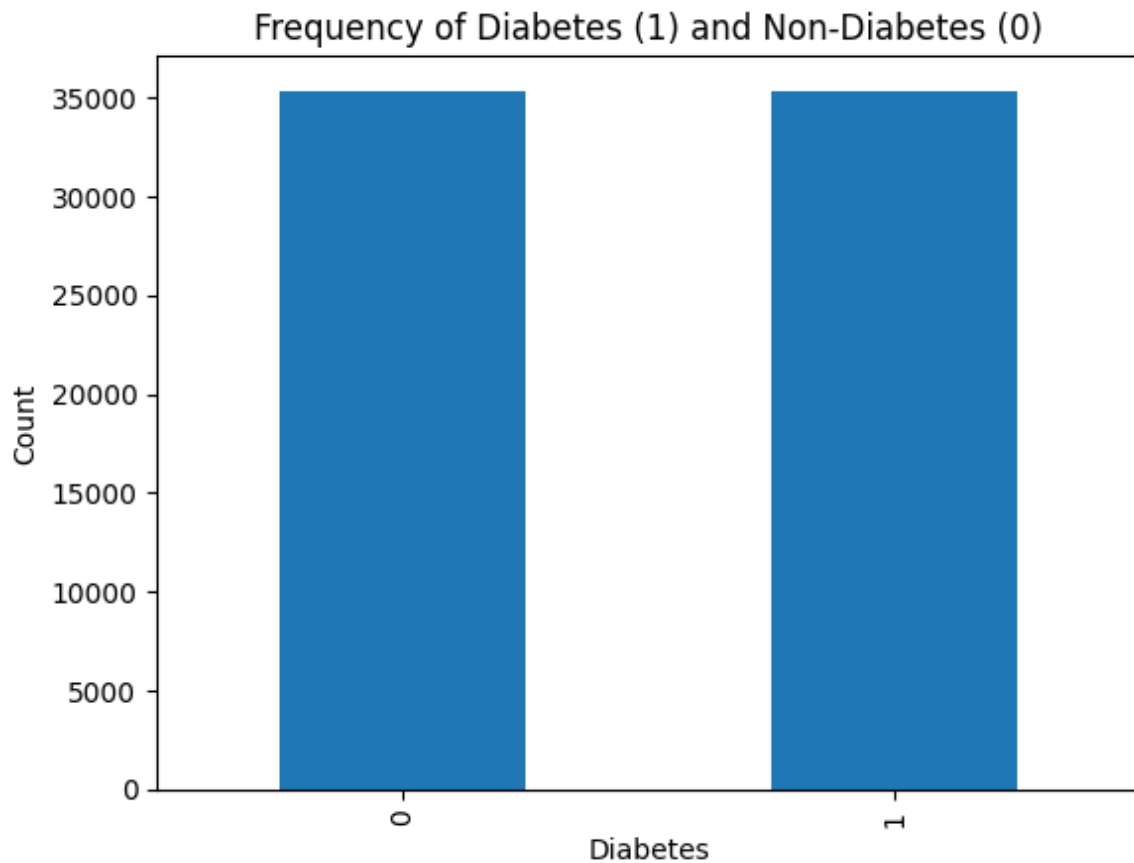


Figure 3. Correlation Heatmap of the Features

Figure 4 shows that there is no class imbalance in the dataset.



**Figure 4.** Frequency of Diabetes (1) and Non-Diabetes (0) Instances in the Dataset

Class imbalance affects negatively on the learning ability of machine learning models. In cases of severe class imbalance, the models prioritize major classes to learn internal data patterns, which lead to poor generalization and performance. Fortunately, dealing with such scenarios is not required in this research.

### 3.3. Model Selection

As mentioned before, three ensemble models are selected for modeling purposes. These models are XGBoost Dart, Light Gradient Boosting Machine (LGBM), and Histogram-based Gradient Boosting Classifier (HistGB). The hyperparameters of these models are tuned with Bayesian Optimization for this task of diabetes diagnosis. Also, a stacked ensemble consisting of the mentioned three ensembles and LGBM as meta-estimator is utilized. This stacked ensemble is trained on causal features. Tabular neural model TabNet is experimentally used to analyze how it performs on diabetes prediction. Uncertainty quantification of the ensemble and causal-guided model is provided. The most optimal model's SHAP interpretation alongside diverse counterfactual explanations (DiCE) is incorporated as well. A brief description of the models is given below.

### 3.4. Light Gradient Boosting Machine (LightGBM)

LightGBM is a highly efficient gradient boosting framework based on decision trees, developed by Microsoft. It is designed to be both faster and more memory-efficient than traditional boosting algorithms due to two key techniques known as Gradient-based One-Side Sampling (GOSS) and Exclusive Feature Bundling (EFB).

LightGBM constructs trees leaf-wise rather than level-wise. The algorithm selects the leaf with the maximum loss reduction at each step. This leads to faster convergence and often better accuracy on

tabular datasets. The objective is to minimize a differentiable loss function  $L(y_i, f(x_i))$  using gradient boosting:

$$f(x) = \sum_{m=1}^M \lambda_m h_m(x), \quad \text{where } h_m(x) \text{ is the base learner}$$

The ensemble is trained sequentially, where weak learner attempts to minimize the residual errors of the previous learners:

$$r_i^{(m)} = - \left[ \frac{\partial L(y_i, f(x_i))}{\partial f(x_i)} \right]_{f=f^{(m-1)}}$$

LightGBM is selected for this work due to its strong performance on tabular data, scalability to large datasets, and compatibility with interpretability tools such as SHAP.

### 3.5. XGBoost DART (Dropout Additive Regression Trees)

XGBoost DART is another ensemble model and a variant of the eXtreme Gradient Boosting (XGBoost) algorithm that incorporates dropout techniques inspired by neural networks in order to prevent overfitting. DART randomly drops a subset of trees while training a new tree, instead of using all the trees in the ensemble at each iteration:

$$f(x) = \sum_{t \in T \setminus D} \lambda_t h_t(x) + h_{\text{new}}(x)$$

Here,  $D$  represents the set of dropped trees, and  $h_{\text{new}}(x)$  is the newly learned regression tree that corrects the bias in the current prediction. The model introduces randomness and regularization into the boosting process to enhance generalization on datasets with potential overfitting. There, XGBoost DART was chosen due to its strong regularization ability, and strong track record in machine learning competitions.

### 3.6. Histogram-Based Gradient Boosting Machine (HistGBM)

Histogram-Based Gradient Boosting is another variant of traditional gradient boosting decision trees (GBDT), where continuous features are first bucketed into discrete bins (histograms). This reduces memory usage and speeds up training by allowing for histogram-based split finding:

$$\text{bin}_j = \left\lfloor \frac{x_j - \min(x)}{\Delta} \right\rfloor, \quad \text{where } \Delta = \frac{\max(x) - \min(x)}{k}$$

Using histogram-based discretization, the model only searches for splits among a fixed number of bins  $k$ , that accelerates computation without sacrificing much accuracy. HistGBM is selected for this task as a faster alternative of previously mentioned gradient boosting models. HistGBM usually has decent computational efficiency and competitive performance, especially when working with medium-sized clinical datasets. It is also supported natively by the `scikit-learn` library, making it easily integrable within cross-validation and pipeline frameworks.

### 3.7. TabNet: Deep Learning with Sparse Attention for Tabular Data

TabNet is a newborn deep neural network architecture tailored for tabular datasets that combines the high performance of deep learning with interpretability, traditionally seen in decision trees. Unlike conventional feed-forward neural networks, TabNet uses a sequential attention mechanism that enables the model to learn which features to focus on at each decision step. This allows for both local interpretability (why the model made a specific decision) and global interpretability (which features are generally important).

## Model Architecture

TabNet operates in multiple decision steps. At each step  $t$ , a feature transformer network processes the input features, and an attention mask  $M^{(t)}$  is generated to determine which features should be emphasized in the current decision step. The overall prediction is formed by aggregating outputs across all decision steps:

$$\hat{y} = \sum_{t=1}^T f_{\text{decision}}^{(t)}(x \odot M^{(t)})$$

where: -  $x$  is the input feature vector, -  $M^{(t)}$  is the sparse attention mask at decision step  $t$ , -  $\odot$  denotes element-wise multiplication (masking), -  $f_{\text{decision}}^{(t)}$  is the transformation block producing output at step  $t$ .

## Sparse Attention and Interpretability

A key novelty of TabNet is its sparse attention mechanism, which enforces that only a subset of input features contribute at each decision step. This is achieved using a learned softmax-based mask over the features with a sparsity-inducing regularization term added to the loss function:

$$\text{Loss} = \text{TaskLoss} + \lambda_{\text{sparse}} \sum_{t=1}^T \sum_{j=1}^d M_j^{(t)} \log M_j^{(t)}$$

This regularization encourages attention distributions  $M^{(t)}$  to be sparse, which turns the model more interpretable by focusing only on the most relevant features. The interpretability can be visualized by aggregating the learned masks across decision steps for each sample (local) or across all samples (global). This makes TabNet particularly suitable for medical diagnosis, where understanding why a prediction was made is critical.

Mathematically, the interpretability in TabNet is achieved through the use of a **sparse attentive mechanism** in its *decision steps*. At each decision step  $i$ , the model applies a learned feature mask  $M^{(i)}$  over the input feature vector  $x$ , where:

$$M^{(i)} = \text{Sparsemax}(P^{(i)} \cdot x)$$

Here,  $P^{(i)}$  is the learnable projection at decision step  $i$ , and the *Sparsemax* activation ensures that the resulting mask is sparse, i.e., it selects only a small subset of features for consideration at each step. This sparse masking enables the model to focus on the most relevant features per sample and per decision step, leading to both efficient learning and built-in interpretability.

The **global feature importance** shown as plot is derived by aggregating these masks across all decision steps and across all training samples. If we denote the aggregated importance of feature  $j$  as:

$$\text{Importance}(j) = \frac{1}{N} \sum_{n=1}^N \sum_{i=1}^T M_{n,j}^{(i)}$$

where  $T$  is the number of decision steps, and  $N$  is the total number of samples, we get a global importance score for each feature. These values reflect how often and how strongly each feature was attended to during the training process.

TabNet is chosen for this study due to its unique combination of:

- **Deep learning power:** Capable of learning complex nonlinear interactions in tabular clinical data.
- **Built-in interpretability:** Sparse attention directly shows which features influenced the model decision.
- **No preprocessing:** Unlike tree-based models, TabNet handles raw numeric and categorical data without the need for heavy preprocessing.

- **Trustworthiness:** Ideal for high-stakes healthcare settings where interpretability and decision transparency are necessary.

Despite having these advantages, TabNet is extremely underutilized in medical domain. Hence, an experimental run and performance evaluation of TabNet on the diabetes data is presented in this paper to align with the recent technological advancements. Moreover, in this work, TabNet's feature masks are analyzed to understand which features were most salient in predicting diabetes for each individual, as well as globally across the cohort. This forms a critical part of the proposed framework's interpretability pipeline.

### 3.8. Causal Inference-Based Feature Selection

With an attempt to identify features with a stable and causal impact on the target variable (Diabetes), the Causal Forest model from the econML library [14] is employed. Each candidate feature was individually treated as a *treatment variable*  $T$ , and its effect on the binary target  $Y$  (presence of diabetes) was estimated using Causal Forests.

The Causal Forest model is based on the potential outcomes framework [15], which assumes that for each individual  $i$ , there exists a potential outcome  $Y_i(t)$  under treatment level  $t$ . The individual treatment effect (ITE) is defined as:

$$\tau_i = Y_i(1) - Y_i(0) \quad (1)$$

Since it is not possible to observe both potential outcomes for the same individual, the *Average Treatment Effect* (ATE) is estimated, which is the expectation over the population:

$$ATE = \mathbb{E}[Y(1) - Y(0)] \quad (2)$$

For continuous treatments, the ATE generalizes to estimating the expected change in outcome per unit change in treatment, while controlling for confounding variables  $X$ . Formally:

$$\tau(X) = \frac{\partial \mathbb{E}[Y|T, X]}{\partial T} \quad (3)$$

To adjust for confounding bias, treatment-specific confounders through a two-step data-driven process are identified:

1. For each candidate treatment variable  $T_j$ , a Random Forest model to predict  $T_j$  using all other features excluding the target  $Y$  and  $T_j$  itself is trained.
2. From the trained model, the top features that cumulatively explained 80% of the total feature importance are selected, denoted by the set  $\mathcal{X}_j$ . These were treated as the confounders for estimating the effect of  $T_j$  on  $Y$ .

Using the Causal Forest DML estimator, the ATE is estimated for each treatment variable  $T_j$  while adjusting for its corresponding confounders  $\mathcal{X}_j$ . Treatment variables that showed an average treatment effect of at least 1% (i.e.,  $ATE_{T_j} \geq 0.01$ ) were considered causally relevant. These features were then selected for inclusion in the stacked ensemble model. The entire process is outlined in Algorithm 1.

**Algorithm 1** Causal Feature Selection with Causal Forests**Require:** Dataset with features  $X = \{T_1, \dots, T_d\}$  and binary target  $Y$ **Ensure:** Selected set of causal features  $\mathcal{T}_{\text{relevant}}$ 

```

1: Initialize  $\mathcal{T}_{\text{relevant}} \leftarrow \emptyset$ 
2: for each feature  $T_j$  in  $X$  do
3:   Train Random Forest to predict  $T_j$  from  $X \setminus \{T_j, Y\}$ 
4:   Identify top features explaining 80% of importance  $\rightarrow \mathcal{X}_j$ 
5:   Estimate ATE of  $T_j$  on  $Y$  using Causal Forest with confounders  $\mathcal{X}_j$ 
6:   if ATE  $\geq 0.01$  then
7:     Add  $T_j$  to  $\mathcal{T}_{\text{relevant}}$ 
8:   end if
9: end for
10: return  $\mathcal{T}_{\text{relevant}}$ 

```

This process makes sure that only features with a causal and stable relationship with the target are used for downstream predictive modeling. This can lead to an improvement in both interpretability and generalizability.

## 4. Results and Discussion

This section provides detailed analysis on model performance, uncertainty, interpretability, and counterfactuals.

### 4.1. Model Evaluation

Table 2 shows the performance comparison of the five models—XGBoost Dart, LightGBM, HistGB, TabNet, and the Causal-Guided Stacked Classifier (CGSC). It reveals distinct strengths and weaknesses across key performance metrics. XGBoost Dart demonstrates robust performance with a precision of 0.76, recall of 0.80, and an F1-score of 0.78, denoting a well-balanced trade-off between identifying true positives and minimizing false positives. The accuracy of the model is 0.78 and AUC is 0.84, which further underscore its reliability as a general-purpose classifier. LightGBM, while exhibiting a slightly lower precision (0.71) and recall (0.76), achieves an exceptional AUC of 0.97, suggesting superior discriminative power in distinguishing between classes, albeit with a marginally lower accuracy of 0.72. HistGB shows moderate performance across all metrics, with precision, recall, and F1-score each hovering around 0.72–0.73, alongside an accuracy of 0.72 and an AUC of 0.78. The ROC-AUC curve of the ensemble models is shown in Figure 5

**Table 2.** Model Performance Comparison

Model	Precision	Recall	F1-Score	Accuracy	AUC
XGBoost Dart	0.76	0.80	0.78	0.78	0.84
LightGBM	0.71	0.76	0.73	0.72	0.97
HistGB	0.72	0.73	0.73	0.72	0.78
TabNet	0.79	0.73	0.76	0.77	0.86
CGSC	0.70	0.81	0.75	0.73	0.80

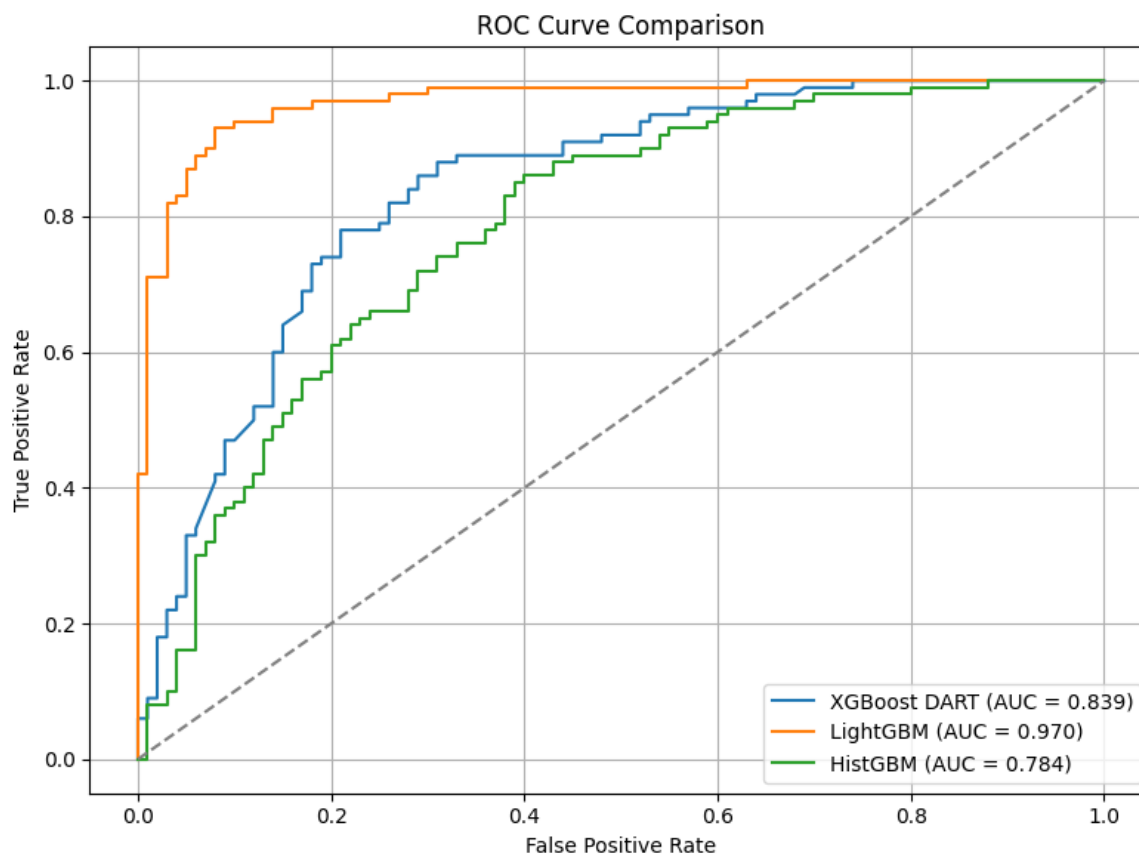


**Figure 5.** ROC-AUC Curve of Three Ensemble Models

TabNet stands out with the highest precision (0.79) among the models. It reflects the model's ability to minimize false positives, though its recall of 0.73 is comparatively lower, that indicates a potential shortfall in capturing all positive instances. Its F1-score of 0.76 and accuracy of 0.77 combined with a strong AUC of 0.86 suggest that is well-suited for applications where precision is paramount. The CGSC model, which integrates Logistic Regression and kNN as base learners with LightGBM as a meta-learner, achieves the highest recall (0.81) but the lowest precision (0.70). This inverse relationship highlights its tendency to prioritize identifying true positives at the cost of increased false positives, which turns it particularly useful in domains like early disease diagnosis where missing a positive case is more detrimental than occasional false alarms. Its F1-score of 0.75 and accuracy of 0.73 are competitive, while its AUC of 0.80 indicates reasonable discriminative capability. Figure 6 illustrates the ROC-AUC curve of these two models.

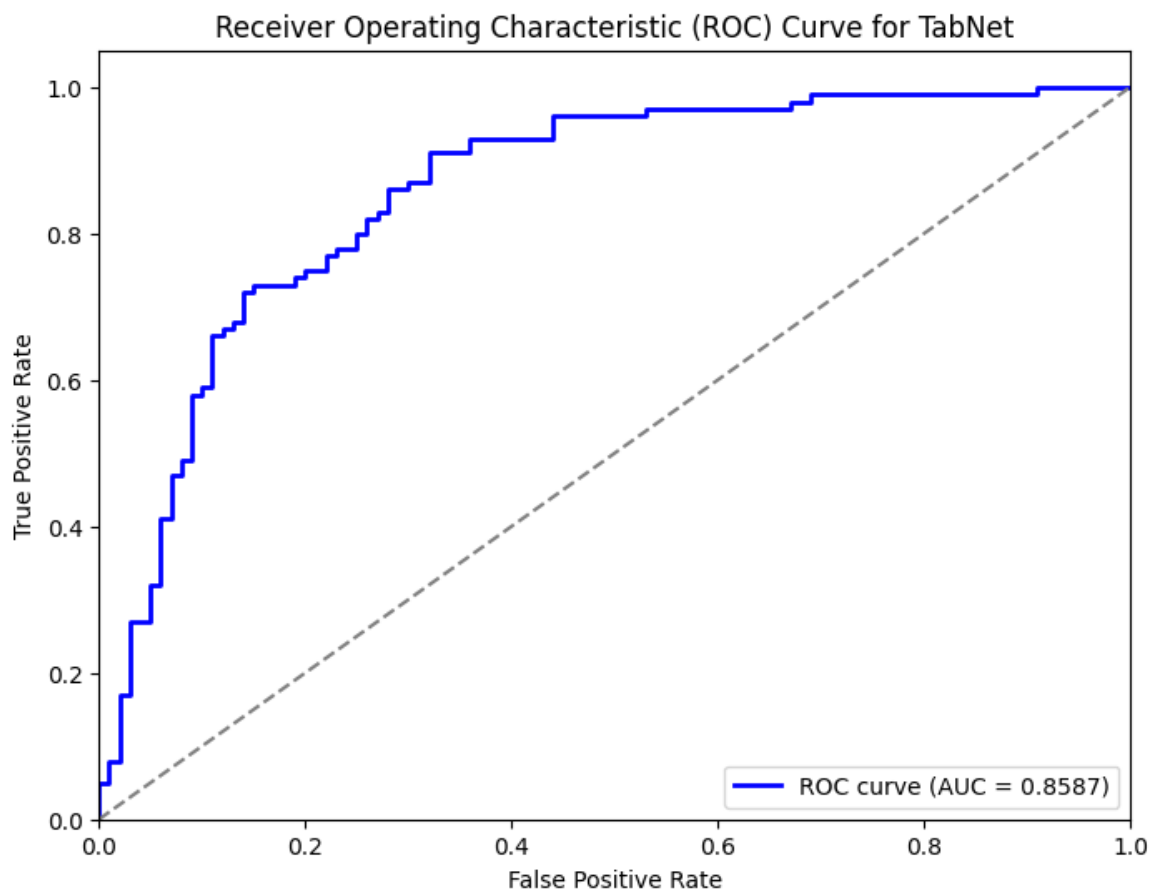
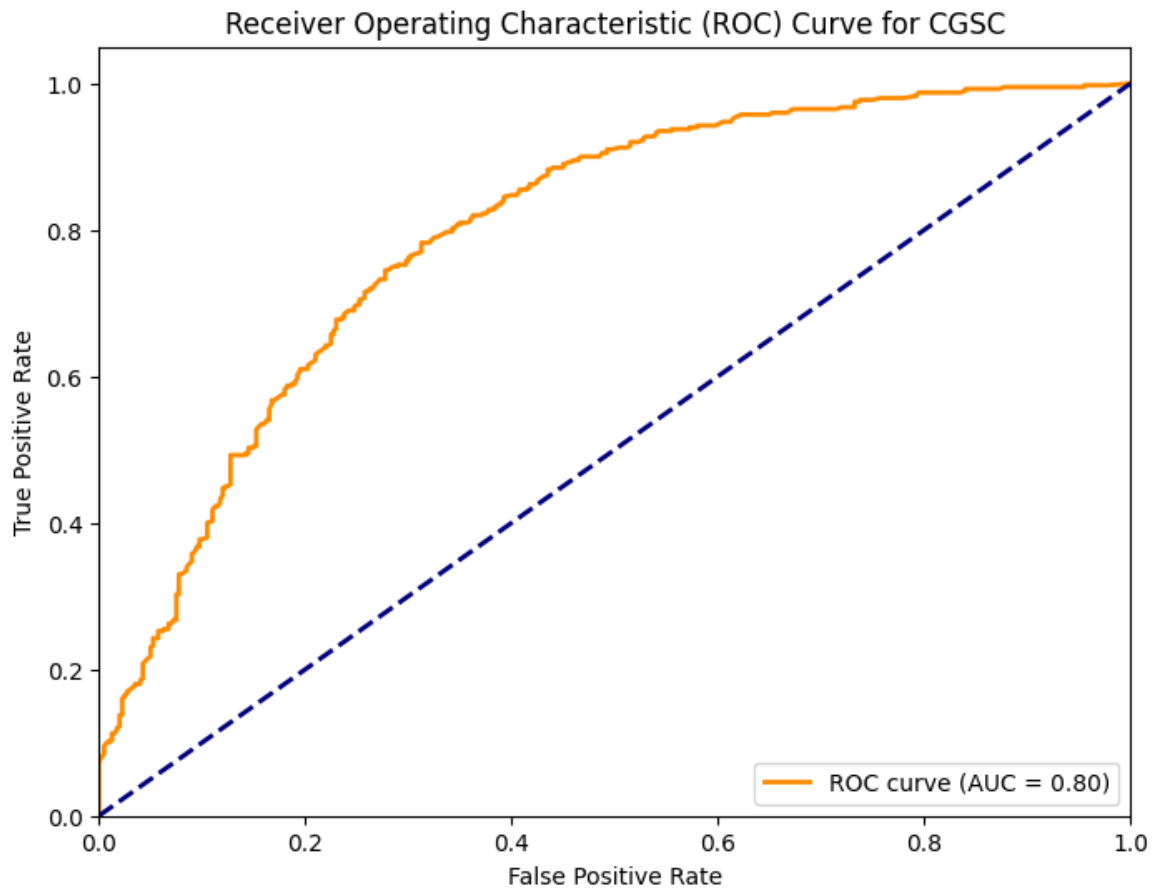
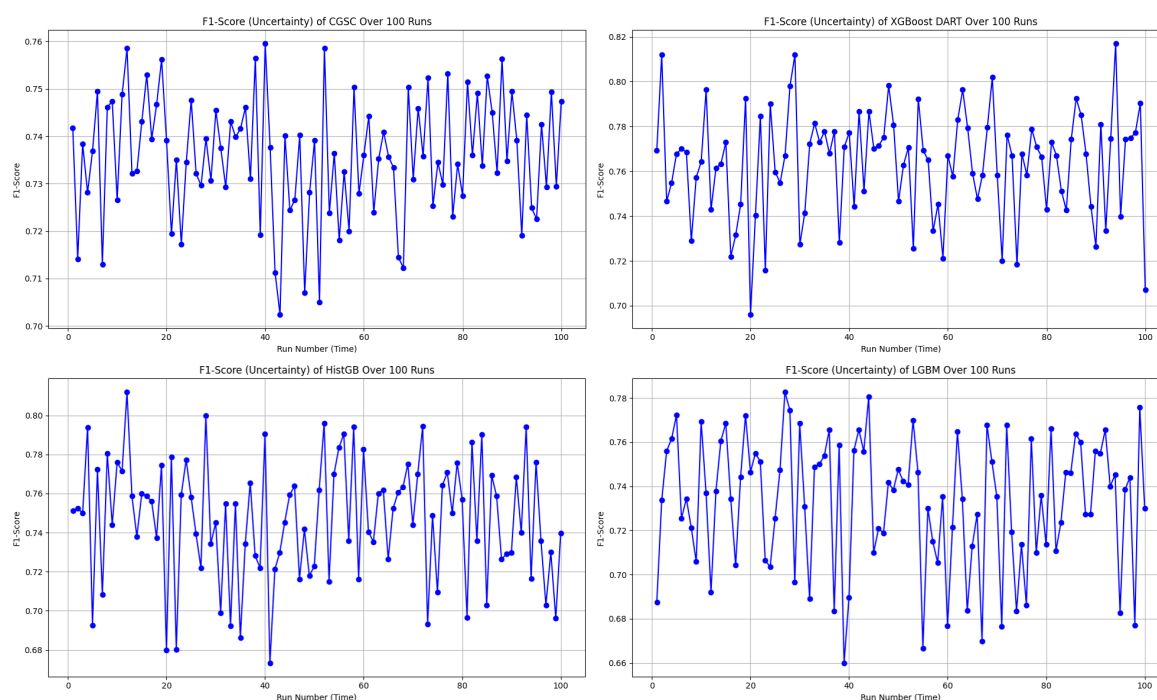


Figure 6. ROC-AUC Curve of TabNet and CGSC

For an early warning diabetes prediction task using non-clinical features, the optimal model should prioritize high recall, good precision, and strong AUC. So, in terms of recall, CGSC is the best model, where for a balanced performance, TabNet and XGBoost shines. However, early warning systems benefit most from high recall as missed cases can lead to preventable complications. CGSC's recall-driven performance aligns best with this goal, while XGBoost provides a safer middle ground if precision cannot be sacrificed entirely.

In the uncertainty plots presented in Figure 7, each of the four models—CGSC, XGBoost DART, HistGB, and LGBM—was evaluated over 100 runs in terms of their F1-score variability.



**Figure 7.** F1-Score Uncertainty of the Ensemble Models

The CGSC model shows a relatively narrow F1-score range of approximately 0.70 to 0.76. Its average performance seems to cluster around 0.735 to 0.74, and although there are a few dips, they are not frequent or severe. This reflects a stable and consistent behavior across repeated executions.

On the other hand, the XGBoost DART model, reaches higher F1-score peaks, ranging from about 0.69 to 0.82, with its mean likely around 0.76 to 0.77. However, the model also exhibits significant fluctuations, that shows frequent drops in performance alongside its high scores. This result suggests a higher variance in behavior which could lead to unpredictable outcomes if not controlled or averaged out.

The HistGB model demonstrates the most erratic performance of the four. Its F1-scores fluctuate between approximately 0.67 and 0.81, with a presumed average close to 0.735. This model suffers from frequent sharp dips and spikes that denotes considerable instability and variance across runs. Such unpredictability could make it less desirable for applications like diabetes diagnosis that requires reliability.

Finally, the LGBM model operates within an F1-score range of roughly 0.66 to 0.78. Its average seems to fall between 0.735 and 0.74, and although it displays performance swings, they are less extreme than those seen in HistGB. Nevertheless, its moderate-to-high variance indicates a certain level of unreliability, albeit to a lesser extent.

Therefore, CGSC emerges as the best option for consistency and robustness in terms of overall preference, with the most stable F1-score across the 100 runs. It performs reliably and avoids dramatic fluctuations, making it well-suited for scenarios where predictability is crucial. Conversely, XGBoost DART delivers the highest individual F1-score performances and could be the optimal choice when

maximizing peak accuracy is a priority, provided that its higher uncertainty is managed—potentially through ensemble methods or additional tuning. HistGB stands out as the least stable model, with its highly volatile performance making it a less favorable choice in most practical settings. LGBM sits between the extremes by showing moderate reliability but not excelling significantly in either consistency or peak performance.

#### 4.2. XGBoost DART Global Interpretability

In order to enhance the transparency and trustworthiness of the diabetes prediction framework, SHAP (SHapley Additive exPlanations) is utilized to interpret the XGBoost DART model globally and locally. SHAP values, grounded in cooperative game theory, attribute a contribution value to each feature by estimating how much each one shifts the model's output from the base value.

The SHAP summary plot in Figure 8 visualizes both the importance and direction of influence of each feature. The horizontal axis represents the SHAP value, which denotes the impact of each feature on the model's prediction. Features are ordered vertically based on their overall contribution across the dataset.

Each point on the plot corresponds to an individual prediction, where the color represents the feature value (red for high, blue for low). A positive SHAP value implies that the feature increases the probability of predicting diabetes, whereas a negative value denotes the opposite.

As observed, **GenHlth (General Health)**, **BMI**, **Age**, and **HighBP (High Blood Pressure)** are the most influential features. Individuals with poor general health (high feature value in red) tend to have positive SHAP values. It explains that they are more likely to be predicted as diabetic. Similarly, higher BMI and older age also contribute positively to the model's prediction. Conversely, higher levels of physical activity (**PhysActivity**) and lower cholesterol levels (**HighChol**) are associated with negative SHAP values. These features act as protective factors.

The model effectively captures non-linear dependencies and feature interactions. For example, even though high blood pressure generally contributes positively to diabetes risk, there are low-value instances (in blue) that occasionally have a small positive SHAP value that reflects contextual interactions with other features.

This global SHAP interpretation validates the clinical plausibility of the model's reasoning and identifies the most salient risk factors for diabetes in the dataset. It also ensures that the model decisions align with domain knowledge, which strengthens its credibility in real-world deployment. However, real-world deployment is beyond the scope of the research for now.

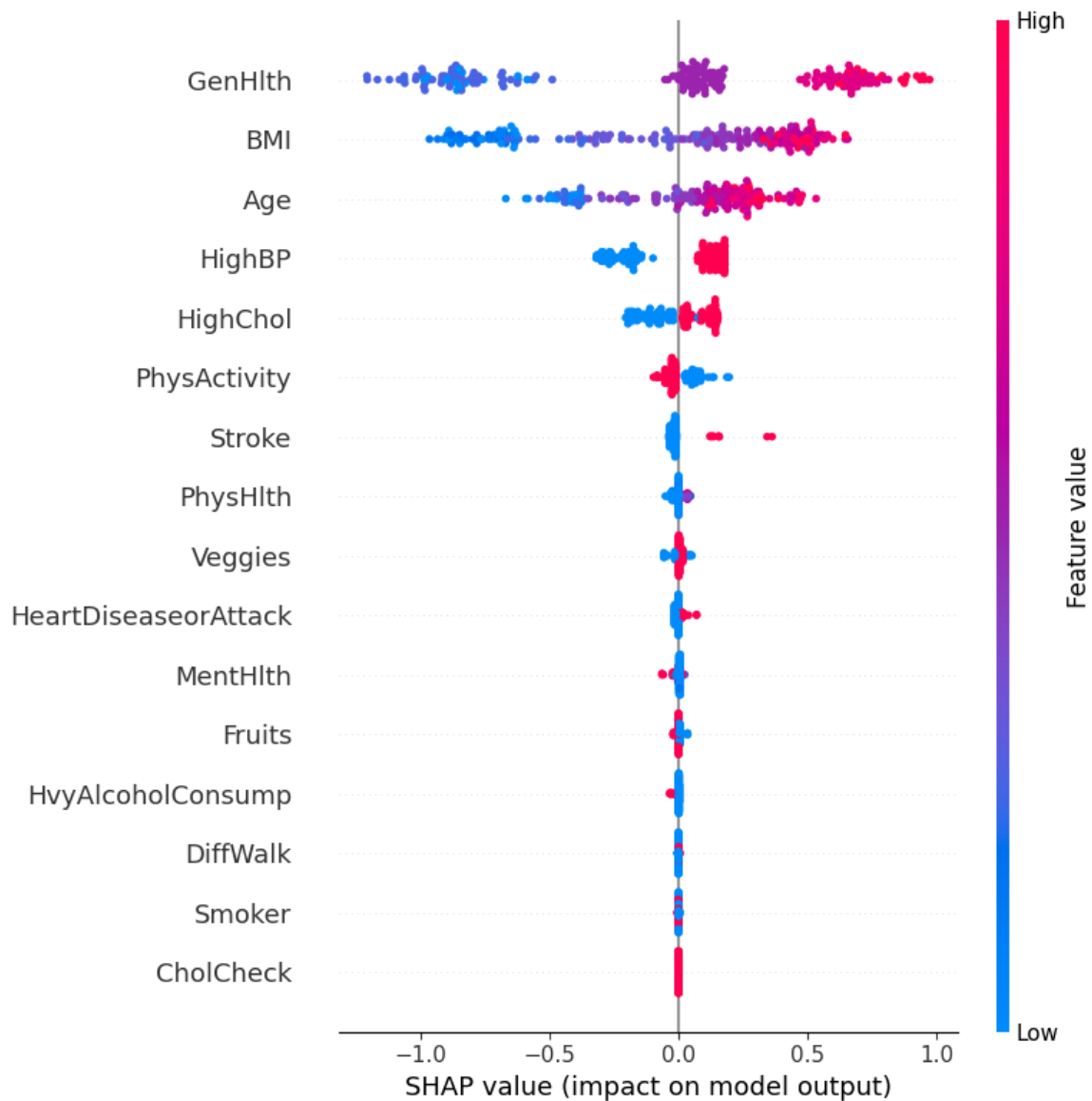


**Figure 8.** SHAP summary plot showing global feature importance and influence direction in the XGBoost DART model for diabetes prediction. Red indicates higher feature values, blue indicates lower values.

#### 4.3. XGBoost Dart Local Interpretability

The model's decision-making process for individual predictions using local SHAP explanations is also investigated to complement the global interpretability analysis. Figure 9 shows a waterfall plot for a single instance that was classified as **not diabetic** (class 0) by the XGBoost DART model.

The SHAP framework decomposes the model output into a sum of contributions from each feature relative to the expected prediction. The expected value of the model output is  $E[f(X)] = 0.188$ . It represents the average model prediction across the dataset. For this specific individual, the final model prediction is  $f(x) = -1.571$ , which strongly pushes the prediction towards the non-diabetic class.

Each bar in the waterfall plot corresponds to a feature's SHAP value contribution. Blue bars indicate features that pushed the prediction lower (towards class 0), whereas red bars indicate features that pushed the prediction higher (towards class 1).

The most influential feature is **BMI**, which contributes  $-0.89$  to the model output, which suggests a relatively low BMI for this individual. This is followed by **General Health (GenHlth)**, which adds another  $-0.79$ , it points to the fact that the person self-reported good general health. **Age** has a slight

positive contribution of +0.3, denoting older age slightly increases the likelihood of diabetes, but not enough to override the strong negative contributions from other features.

Other negative contributors include **HighBP** (−0.17), **HighChol** (−0.11), and **PhysActivity** (−0.05), suggesting that the individual does not have high blood pressure or cholesterol and is physically active—all of which are consistent with a lower risk of diabetes. The remaining features such as **Stroke**, **HeartDiseaseorAttack**, and **PhysHlth** also have slight contributions.

This localized interpretation ensures transparency at the individual level that confirms the alignment of model's prediction with clinical reasoning. It further enables trust in model deployment, especially in sensitive healthcare settings where individualized decisions matter.

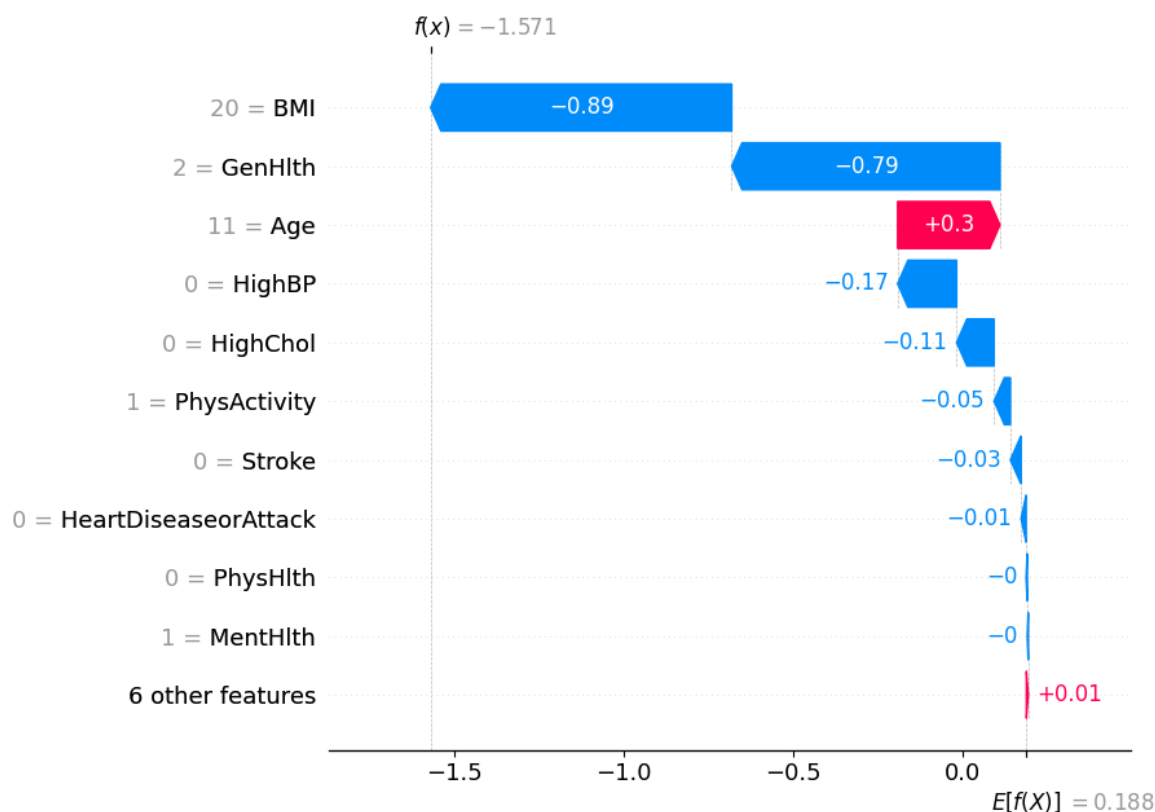


**Figure 9.** Local SHAP explanation from XGBoost DART for an individual predicted as not diabetic (class 0). Each bar represents the feature's contribution to pushing the model output away from the base value  $E[f(X)] = 0.188$  toward the final prediction  $f(x) = -1.571$ .

Similarly, the local SHAP explanation illustrated in Figure 10 corresponds to an individual who was predicted as **diabetic** (class 1) by the XGBoost DART model. The model's expected output is  $E[f(X)] = 0.188$ , whereas the final prediction for this instance is significantly higher,  $f(x) = 0.822$ , indicating a high likelihood of diabetes.

The feature with the highest positive contribution is **General Health (GenHlth)**, which adds +0.6 to the prediction. This suggests the individual reported poor general health that is indeed a strong risk factor associated with diabetes. **BMI** also positively contributes +0.39 that implies an elevated body mass index, another major risk indicator. Although **Age** contributes negatively (−0.38), as category 5 reflects a younger age, this is outweighed by the stronger positive contributions.

Additional features such as **HighBP** (+0.1), **PhysActivity** (+0.07), and **PhysHlth** (+0.03) also pull the prediction higher. This insight suggests an association of limited physical activity or physical health issues with diabetes risk. Conversely, **HighChol** contributes negatively, it indicates that normal cholesterol somewhat mitigated the prediction, though not enough to change the final outcome.

This SHAP plot reaffirms the model's decision in an interpretable manner, showcasing how combinations of risk factors (particularly poor general health and high BMI) drive a high-confidence diabetes prediction.

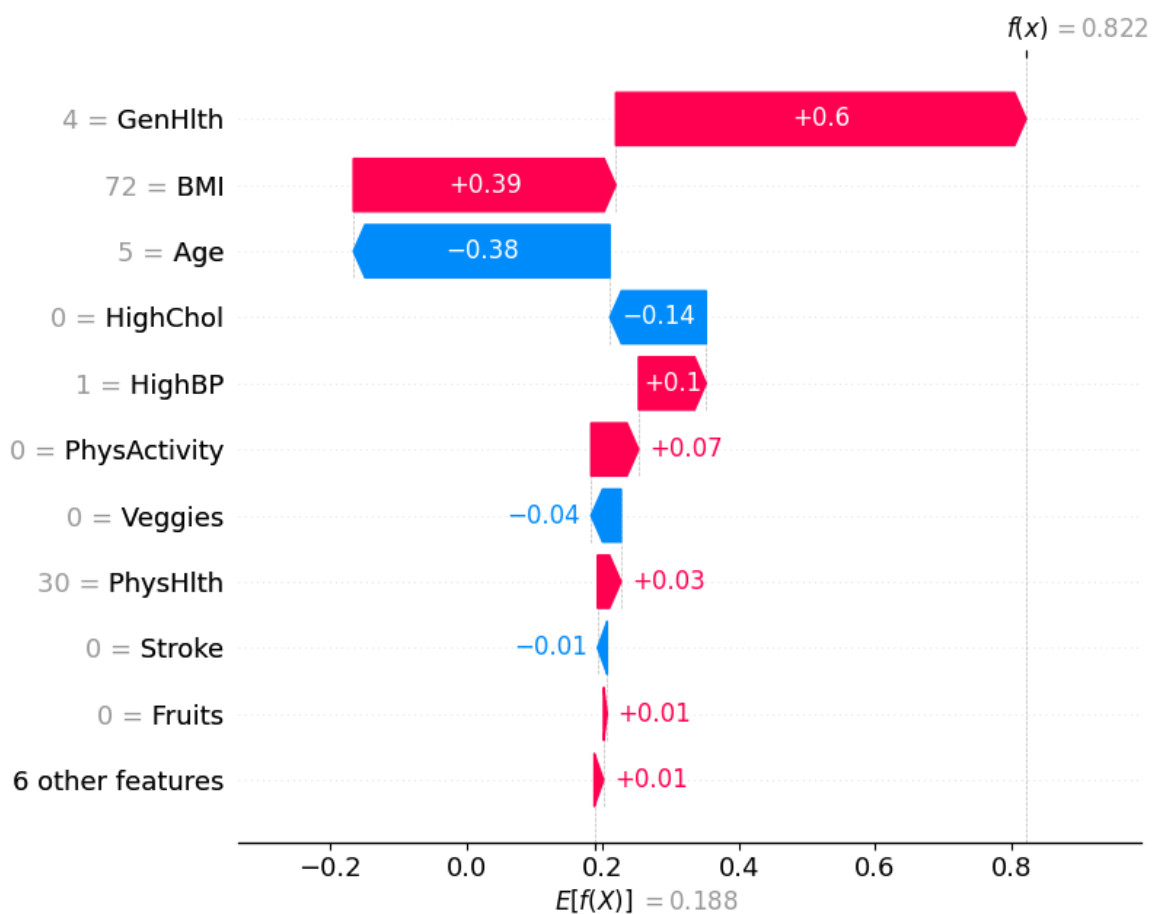


**Figure 10.** Local SHAP explanation from XGBoost DART for an individual predicted as diabetic (class 1). Each feature's SHAP value shows its influence in moving the prediction from the expected base value  $E[f(X)] = 0.188$  to the final output  $f(x) = 0.822$ .

#### 4.4. TabNet Global Interpretability

The bar chart provided in Figure 11 visualizes the global feature importance scores generated by TabNet. The x-axis represents the importance score which is a normalized value that sums to 1 across all features, and the y-axis lists the input features used in the model. The longer the bar, the more frequently or more significantly the feature was used in TabNet's decision-making process.

From the plot, the feature GenHlth (General Health) has the highest importance score which explains that the model relies heavily on this feature when predicting the likelihood of diabetes. This makes sense in a healthcare context since general health status often correlates with chronic conditions like diabetes.

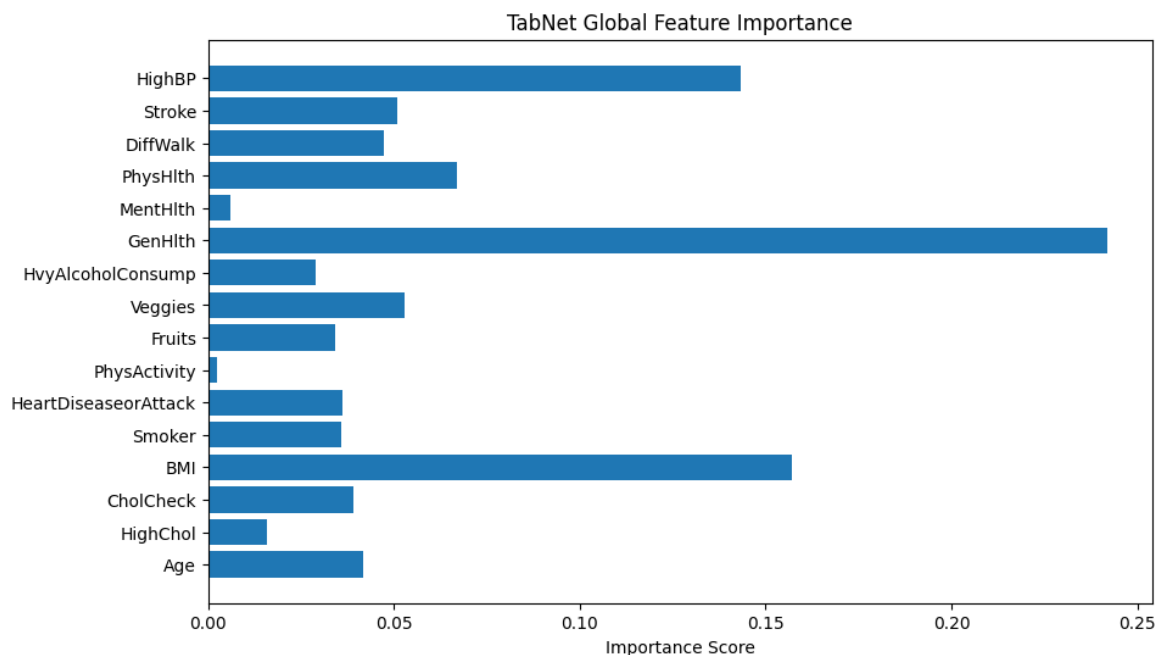


**Figure 11.** Global Feature Importance by TabNet

BMI and HighBP (high blood pressure) are also highly weighted, consistent with known risk factors for diabetes. On the other hand, features such as PhysActivity and MentHlth have very low importance scores. It implies that they contribute little to the predictive power for early warning of diabetes. The global feature importance in TabNet provides both an interpretable and theoretically grounded summary of which input features influence the model's decisions. Fortunately, interpretability lead by the sparse attention mechanism is intrinsic to the model architecture and does not require post hoc explanations like SHAP or LIME. As a result, it is possible to directly trust the attribution scores to guide feature selection, model understanding, or communication of results to domain experts.

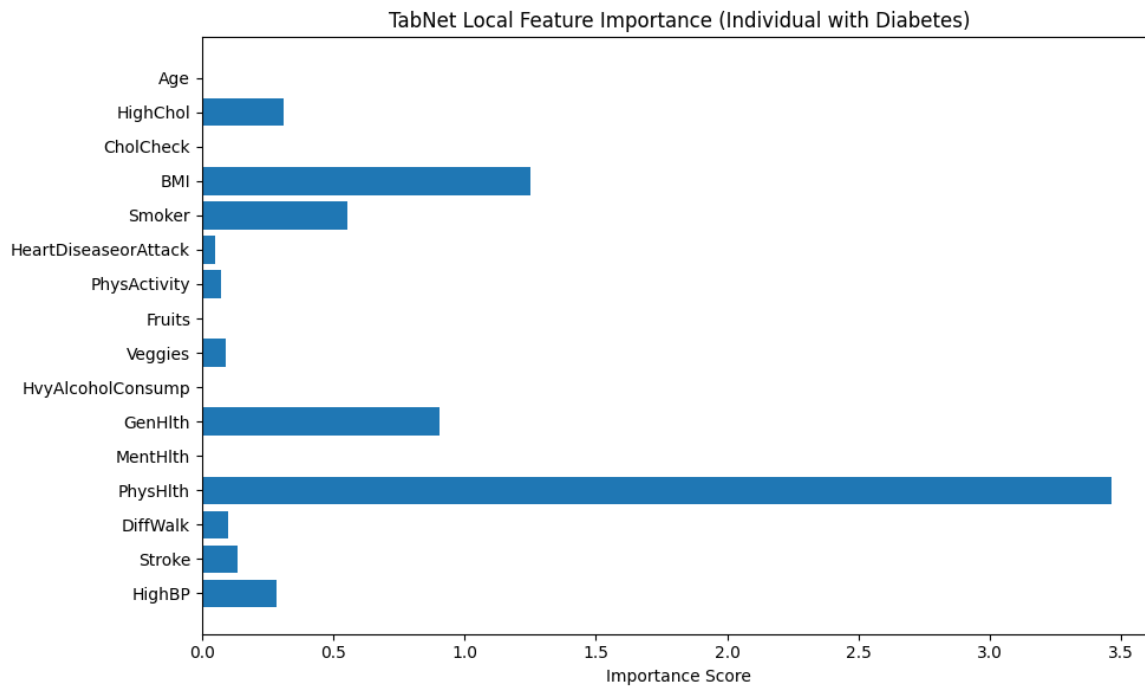
#### 4.5. TabNet Local Interpretability

Figure 12 illustrates the local feature importance derived from a TabNet model when predicting an instance as diabetic (class 1). The horizontal bar plot displays the importance scores of each input feature. It mentions how significantly each feature contributed to the model's decision for this particular individual.

From the plot, it is explicit that **PhysHlth** (Physical Health) is the most influential feature in the model's prediction, with an importance score approaching 3.5. This suggests that the number of physically unhealthy days reported by the individual played a dominant role in classifying them as diabetic. The next most impactful features are **BMI** (Body Mass Index) and **GenHlth** (General Health), which denotes that higher body mass and poorer self-rated general health are also critical in determining diabetes presence for this subject.

Other features with notable contributions include **Smoker** and **HighBP** (High Blood Pressure), which align with known risk factors for diabetes. The variables **HighChol**, **DiffWalk** (Difficulty Walking), and **MentHlth** (Mental Health) show moderate influence, suggesting some relationship but to a lesser extent.

Features such as **Age**, **CholCheck**, **PhysActivity**, **Fruits**, **Veggies**, **HvyAlcoholConsump**, and **HeartDiseaseorAttack** contributed minimally in this individual case. These variables may be important at a population level, but their low scores here indicate limited relevance in the model's specific decision for this person.



**Figure 12.** TabNet Local Feature Importance Plot for an Individual Classified as Diabetic

This analysis emphasizes the personalized interpretability provided by TabNet that adapts the contribution of features based on the unique characteristics of the individual case. It allows for more precise clinical insights and decision-making support.

On the other hand, Figure 13 illustrates the local feature importance scores generated by the TabNet model for an individual who was classified as not having diabetes. This interpretation allows us to examine which features contributed most significantly to the model's prediction for this specific instance.

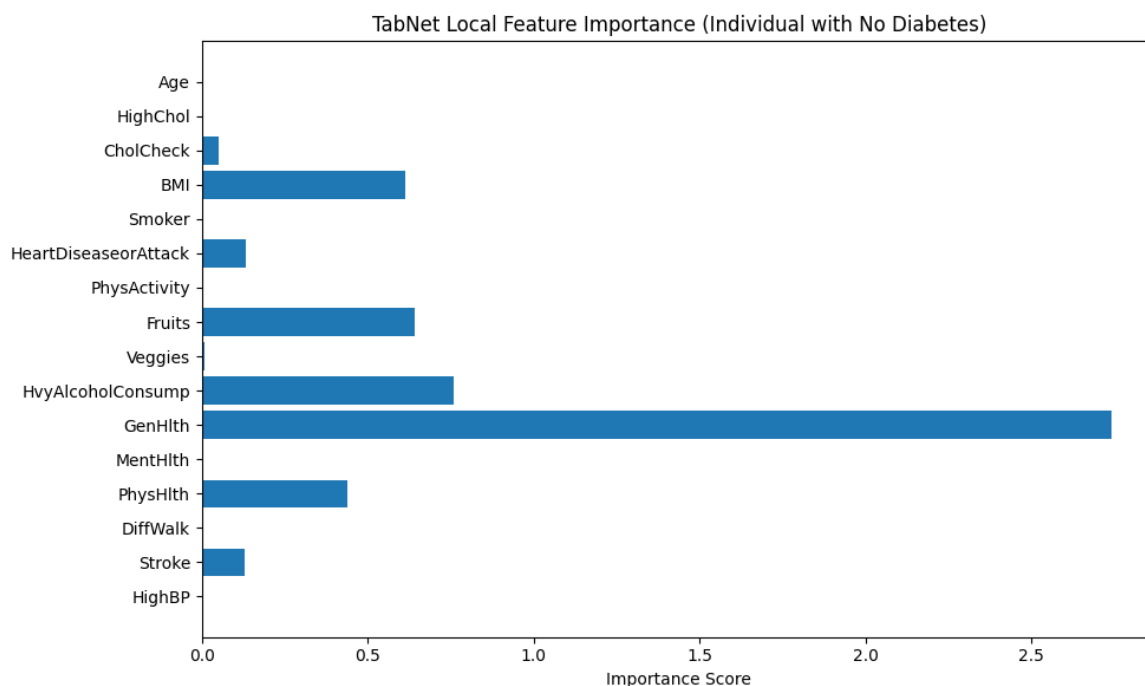


**Figure 13.** TabNet Local Feature Importance for an Individual Predicted as Non-Diabetic

Among all features, *GenHlth* (General Health) holds the highest importance score by a considerable margin, indicating that the individual's self-reported general health status played a dominant role in

the model's decision. The importance score for *GenHlth* exceeds 2.7, far surpassing that of any other feature, which suggests that better perceived general health likely contributed to the classification as non-diabetic. Other features with moderate importance include *HvyAlcoholConsump* (Heavy Alcohol Consumption), *Fruits* (fruit intake), and *BMI* (Body Mass Index), have importance scores ranging approximately between 0.6 and 0.8. These features likely provided additional evidence supporting the non-diabetic classification, possibly by aligning with healthier lifestyle patterns or lower obesity risk. Additional contributions came from *PhysHlth* (Physical Health) and *HeartDiseaseorAttack*, though their influence was lower in magnitude. Interestingly, features such as *HighBP* (High Blood Pressure), *Stroke*, *Smoker*, and *PhysActivity* registered negligible or near-zero importance, pointing to the fact that they did not influence the model's decision for this particular instance.

This localized explanation highlights TabNet's ability to assign dynamic importance to features based on the specific characteristics of the input data. In this case, it shows a heavy reliance on self-reported health and lifestyle indicators over clinical history or demographic information when predicting the absence of diabetes.

#### 4.6. Diverse Counterfactual Explanations

DiCE (Diverse Counterfactual Explanations) framework is employed to better understand the decision boundary of the predictive model. Figure 14 presents a counterfactual analysis where the goal was to identify minimal yet diverse feature changes that would alter the prediction of a given individual from non-diabetic (class 0) to diabetic (class 1).

The first row of the table corresponds to the original instance classified as non-diabetic. Notably, this individual has a low *BMI* of 20.0, does not suffer from high blood pressure, stroke, or walking difficulties, and reports excellent general health (*GenHlth* = 0.0, indicating "excellent"). The physical health burden (*PhysHlth*) is minimal, and lifestyle indicators such as *PhysActivity* and *Fruits* intake appear favorable.

	Age	HighChol	CholCheck	BMI	Smoker	HeartDiseaseorAttack	PhysActivity	Fruits	Veggies	HvyAlcoholConsump	GenHlth	MentHlth	PhysHlth	Diffwalk	Stroke	HighBP	Diabetes
0	11.0	0.0	1.0	20.0	1.0	0.0	1.0	0.0	1.0	0.0	2.0	1.0	0.0	0.0	0.0	0.0	0
Diverse Counterfactual set (new outcome: 1)																	
	Age	HighChol	CholCheck	BMI	Smoker	HeartDiseaseorAttack	PhysActivity	Fruits	Veggies	HvyAlcoholConsump	GenHlth	MentHlth	PhysHlth	Diffwalk	Stroke	HighBP	Diabetes
0	11.0	0.0	1.0	72.2	1.0	0.0	1.0	0.0	1.0	0.6	2.0	1.0	0.0	0.0	0.0	0.0	1
1	11.0	0.0	1.0	58.7	1.0	0.0	1.0	0.0	1.0	0.0	2.0	1.0	14.3	0.0	0.0	0.0	1
2	11.0	0.0	1.0	71.6	1.0	0.0	1.0	0.0	1.0	0.0	2.0	1.0	0.0	0.0	0.0	0.0	1

**Figure 14.** Counterfactual examples generated by DiCE showing minimal changes needed to alter a prediction from non-diabetic (0) to diabetic (1)

The subsequent rows display counterfactual examples that lead to a prediction of diabetes (class 1) while keeping most features constant. Across all three counterfactuals, the feature *BMI* increases dramatically, in one case reaching as high as 72.2, which indicates morbid obesity. This is the most prominent change and a likely causal factor in the altered prediction. In one counterfactual, there is also a significant rise in the *PhysHlth* score (14.3), suggesting more days of poor physical health in the past month, which contributes further to the risk profile.

Interestingly, features like *Age*, *Smoker*, *HeartDiseaseorAttack*, and *HighBP* remain unchanged, emphasizing that for this particular individual, obesity and physical health degradation alone were sufficient to flip the classification.

This counterfactual analysis supports the earlier local interpretability findings by reinforcing the high sensitivity of the model to variables like *BMI*, and *PhysHlth*. Moreover, it provides actionable insights that indicates that substantial weight gain and declining physical condition could move an individual from a non-diabetic to a diabetic risk category in the model's view.

Figure 15 presents examples on counterfactual instances that would flip the prediction to non-diabetic (class 0) from diabetic (class 1).

The original individual is classified as diabetic and exhibits extremely high *BMI* (72). This high body mass index is a consistent factor driving the diabetic classification. Additional characteristics

such as lack of physical activity (*PhysActivity* = 0), poor general health (*GenHlth* = 4), and elevated physical health burden (*PhysHlth* up to 30) further reinforce the model's diabetic prediction.

	Age	HighChol	CholCheck	BMI	Smoker	HeartDiseaseorAttack	PhysActivity	Fruits	Veggies	HvyAlcoholConsump	GenHlth	MentHlth	PhysHlth	DiffWalk	Stroke	HighBP	Diabetes
0	5.0	0.0	1.0	72.0	0.0	0.0	0.0	0.0	0.0	0.0	4.0	0.0	30.0	1.0	0.0	1.0	1
Diverse Counterfactual set (new outcome: 0)																	
	Age	HighChol	CholCheck	BMI	Smoker	HeartDiseaseorAttack	PhysActivity	Fruits	Veggies	HvyAlcoholConsump	GenHlth	MentHlth	PhysHlth	DiffWalk	Stroke	HighBP	Diabetes
0	5.0	0.0	1.0	72.0	0.0	0.0	0.0	0.0	0.0	0.0	2.3	0.0	22.3	1.0	0.0	1.0	0
1	5.0	0.0	1.0	72.0	0.0	0.0	0.9	0.0	0.0	0.0	2.7	0.0	30.0	1.0	0.0	1.0	0
2	5.0	0.0	1.0	14.5	0.0	0.0	0.0	0.0	0.0	0.0	4.0	0.0	26.6	1.0	0.0	1.0	0

**Figure 15.** Counterfactual examples generated by DiCE showing how an individual classified as diabetic (1) could instead be classified as non-diabetic (0) through a reduction in BMI.

Among the three counterfactual instances that revert the outcome to non-diabetic, the third counterfactual shows a drastic reduction in *BMI* from these elevated levels down to a healthy value of 14.5. *PhysHlth* also is slightly reduced to 26.6 (27) from 30. These changes appears sufficient to alter the model's classification. Notably, all other features remain unchanged, including lifestyle factors such as *Smoker*, *PhysActivity*, and *HvyAlcoholConsump*, as well as clinical history like *HighBP*, *Stroke*, and *HeartDiseaseorAttack*.

This finding suggests that, for this individual, body mass index is a critical determinant in the model's assessment of diabetes risk. The fact that only a reduction in *BMI* leads to a change in outcome underscores the model's strong sensitivity to obesity-related features. It also reinforces the conclusion from the local feature importance analysis and previous counterfactuals, where *BMI* consistently emerged as a pivotal variable. Such analysis not only provides interpretability but also offers actionable insight: weight reduction alone might suffice to transition an individual's model-based diabetes risk profile from high to low, at least from the model's perspective.

#### 4.7. Causal Inference

Table 3 presents the Average Treatment Effect (ATE) for each feature, sorted by their absolute values. This allows identification of both strong positive and negative contributors to diabetes prediction.

**Table 3.** Average Treatment Effect (ATE) of Features (Sorted by Absolute Value)

Feature	ATE
CholCheck	0.2583
Alcohol	-0.1875
Genhlt	0.1392
Heart disease	0.1336
Stroke	0.1258
HighChol	0.0975
HighBP	0.0779
Diffwalk	0.0716
Age	0.0260
BMI	0.01589
PhysAct	0.00457
Smoker	-0.0022
Fruits	-0.0011
Mentlhl	-0.0007
Veg	0.0011
Physhlt	0.0003

The table presents that, on average, one unit increase (health decreasing one unit) in **Genhlt** increases the probability of diabetes by 13.92%, adjusting the corresponding confounders. Similarly, if the individual ever suffered from heart disease or stroke, the probability of diabetes increases by 13.36% and 12.58% respectively. Increment of high cholesterol and high blood pressure also increases the chances of diabetes by 9.75% and 7.79% respectively. Surprisingly, an ATE of -0.1875 for the Alcohol

feature means that individuals with high alcohol consumption (value = 1) are, on average, 18.75% points less likely to be predicted as diabetic compared to those with low alcohol consumption (value = 0), controlling for all other confounders. This result may appear counterintuitive, which raises a few possibilities such as confounding effects (younger, healthier individuals might also report higher alcohol use), selection bias (perhaps heavy drinkers underreport symptoms or do not get diagnosed), or measurement issues or reverse causality (people with diabetes might reduce drinking). It is also can be noticed that checking up on cholesterol is associated with 25.83% points increase in the probability of diabetes. However, it does not mean that checking cholesterol causes diabetes. Rather, individuals who are at risk, have symptoms, or have comorbidities are more likely to undergo such screenings.

## 5. Conclusion

A trustworthy machine learning framework for early warning of diabetes is proposed in this research by integrating causal inference, modern ensembles (LightGBM, XGBoost-DART, HistGBM), and TabNet for tabular deep learning. The Causal-guided Stacking Classifier (CGSC) achieved the highest recall (0.81), while TabNet excelled in precision (0.79). Causal Forests identified stable predictors, SHAP provided interpretability for ensembles, and TabNet's sparse attention mechanism offered intrinsic explanations, whereas counterfactual analysis (DiCE) enabled actionable risk mitigation insights. Uncertainty quantification on the other hand confirmed model stability. An attempt is also made to mitigate bias by excluding gender during modeling in order to add transparency and fairness to the model. Future work could enhance more robust fairness integration and real-world deployment for early warning of diabetes. Furthermore, extensive causal inference analysis can be conducted to shed light on the counterintuitive results achieved from this research.

## References

1. International Diabetes Federation. (2021). IDF Diabetes Atlas (10th ed.). Retrieved from <https://diabetesatlas.org>
2. World Health Organization. (2021). Diabetes. <https://www.who.int/news-room/fact-sheets/detail/diabetes>
3. Zhou, B., Lu, Y., Hajifathalian, K., Bentham, J., Di Cesare, M., Danaei, G., ... & Ezzati, M. (2020). Worldwide trends in diabetes since 1980: A pooled analysis of 751 population-based studies with 4.4 million participants. *The Lancet*, 387(10027), 1513–1530. [https://doi.org/10.1016/S0140-6736\(16\)00618-8](https://doi.org/10.1016/S0140-6736(16)00618-8)
4. Forouhi, N. G., & Wareham, N. J. (2019). Epidemiology of diabetes. In *International Textbook of Diabetes Mellitus* (pp. 23–34). Wiley Blackwell. <https://doi.org/10.1002/9781119043702.ch2>
5. Tabák, A. G., Herder, C., Rathmann, W., Brunner, E. J., & Kivimäki, M. (2012). Prediabetes: A high-risk state for diabetes development. *The Lancet*, 379(9833), 2279–2290. [https://doi.org/10.1016/S0140-6736\(12\)60283-9](https://doi.org/10.1016/S0140-6736(12)60283-9)
6. Beam, A. L., & Kohane, I. S. (2020). *Big data and machine learning in health care*. *JAMA*, 324(11), 1033–1034. <https://doi.org/10.1001/jama.2020.11265>
7. American Diabetes Association. (2023). Standards of Medical Care in Diabetes—2023 Abridged for Primary Care Providers. *Clinical Diabetes*, 41(1), 4–31. <https://doi.org/10.2337/cd23-as01>
8. Bonora, E., & Tuomilehto, J. (2011). The pros and cons of diagnosing diabetes with A1C. *Diabetes Care*, 34(2), S184–S190. <https://doi.org/10.2337/dc11-s219>
9. Basu, S., Sussman, J. B., Rigdon, J., Steimle, L., & Hayward, R. A. (2018). Personalized diabetes screening strategies: A cost-effectiveness analysis. *Annals of Internal Medicine*, 169(1), 1–10. <https://doi.org/10.7326/M17-1802>
10. Kengne, A. P., Echouffo-Icheugui, J. B., Sobngwi, E., & Mbanya, J. C. (2013). New insights on diabetes mellitus and obesity in Africa—Part 1: Prevalence, pathogenesis and comorbidities. *Heart*, 99(14), 979–983. <https://doi.org/10.1136/heartjnl-2012-303029>
11. Griffin, S. J., Little, P. S., Hales, C. N., Kinmonth, A. L., & Wareham, N. J. (2000). Diabetes risk score: Towards earlier detection of type 2 diabetes in general practice. *Diabetes/Metabolism Research and Reviews*, 16(3), 164–171. [https://doi.org/10.1002/1520-7560\(200005/06\)16:3<164::AID-DMRR94>3.0.CO;2-0](https://doi.org/10.1002/1520-7560(200005/06)16:3<164::AID-DMRR94>3.0.CO;2-0)
12. Contreras, I., & Vehi, J. (2016). Artificial intelligence for diabetes management and decision support: Literature review. *Journal of Medical Internet Research*, 18(11), e163. <https://doi.org/10.2196/jmir.5780>

13. Shickel, B., Tighe, P. J., Bihorac, A., & Rashidi, P. (2017). Deep EHR: A survey of recent advances in deep learning techniques for electronic health record (EHR) analysis. *IEEE Journal of Biomedical and Health Informatics*, 22(5), 1589–1604. <https://doi.org/10.1109/JBHI.2017.2767063>
14. Microsoft Research. (2020). *EconML: A Python package for estimating causal effects in ML settings*. Retrieved from <https://github.com/microsoft/EconML>
15. Rubin, D. B. (1974). Estimating causal effects of treatments in randomized and nonrandomized studies. *Journal of Educational Psychology*, 66(5), 688–701. <https://doi.org/10.1037/h0037350>
16. Rajkomar, A., Hardt, M., Howell, M. D., Corrado, G., & Chin, M. H. (2019). Ensuring fairness in machine learning to advance health equity. *Annals of Internal Medicine*, 169(12), 866–872. <https://doi.org/10.7326/M18-1990>
17. Caruana, R., Lou, Y., Gehrke, J., Koch, P., Sturm, M., & Elhadad, N. (2015). Intelligible models for healthcare: Predicting pneumonia risk and hospital 30-day readmission. In *Proceedings of the 21st ACM SIGKDD International Conference on Knowledge Discovery and Data Mining* (pp. 1721–1730). <https://doi.org/10.1145/2783258.2788613>
18. Ghosh, P., & Argal, L. (2024). Uncovering Hidden Patterns for Diabetes Prediction: A Synergy of EDA and Ensemble Learning. *International Journal of Engineering and Advanced Scientific Research*, ResearchGate. Retrieved from <https://www.researchgate.net/publication/391220334>
19. Kirubakaran, S., Golla, V., & Sivarajakumar, D. (2025). A Qualitative Investigation of Efficacy of Fuzzy Support Employing Vector Regression in Progressive Diabetes Identification. In *International Conference on Soft Computing and Pattern Recognition* (pp. 498–505). Springer. [https://doi.org/10.1007/978-3-031-81080-0\\_47](https://doi.org/10.1007/978-3-031-81080-0_47)
20. Alkhalidi, M., Khuoj, A., Almsfer, M., Alshulail, B., & Abudalfa, S. (2025). Machine Learning for Early Detection of Type 2 Diabetes Based on Liver Enzymes and BMI. In *Sustainable Data Management* (pp. 293–301). Springer. [https://doi.org/10.1007/978-3-031-83915-3\\_23](https://doi.org/10.1007/978-3-031-83915-3_23)
21. Meng, Z., Guan, Z., Yu, S., Wu, Y., Zhao, Y., Shen, J., & Zhang, Y. (2025). Non-invasive biopsy diagnosis of diabetic kidney disease via deep learning applied to retinal images: a population-based study. *The Lancet Digital Health*. [https://www.thelancet.com/journals/landig/article/PIIS2589-7500\(25\)00040-8/fulltext](https://www.thelancet.com/journals/landig/article/PIIS2589-7500(25)00040-8/fulltext)
22. Sushith, M., Sathiya, A., Kalaipoonguzhali, V., & Sathya, V. (2025). A hybrid deep learning framework for early detection of diabetic retinopathy using retinal fundus images. *Scientific Reports*. <https://www.nature.com/articles/s41598-025-99309-w>
23. Xiao, Z., Wang, M., Zhao, Y., & Wang, H. (2025). A Biomarker-Driven and Interpretable Machine Learning Model for Diagnosing Diabetes Mellitus. *Food Science & Nutrition*, Wiley. <https://onlinelibrary.wiley.com/doi/10.1002/fsn3.70234>
24. Wang, N., Jin, Y., Zhao, Z., Wu, Q., Li, F., & Wang, X. (2025). Study on Classification Detection Method of Diabetic Retinopathy Based on SSD. *Sensing and Imaging*, Springer. <https://doi.org/10.1007/s11220-025-00578-6>
25. Gupta, V., Dash, Y., Sarangi, S. C., & Abraham, A. (2025). Quantum Transfer Learning for Enhanced Diabetic Retinopathy Detection Using ResNet Architecture. In *Soft Computing and Pattern Recognition* (pp. 562–571). Springer. [https://doi.org/10.1007/978-3-031-81080-0\\_53](https://doi.org/10.1007/978-3-031-81080-0_53)
26. Ge, J., Sun, S., Zeng, J., Jing, Y., Ma, H., & Qian, C. (2025). Development and validation of machine learning models for predicting low muscle mass in patients with obesity and diabetes. *Lipids in Health and Disease*. <https://doi.org/10.1186/s12944-025-02577-8>
27. Hasan, K. S. (2025). *Diabetes-Early-Warning* [Computer Software]. GitHub. <https://github.com/SakibHasanSimanto/Diabetes-Early-Warning>

**Disclaimer/Publisher’s Note:** The statements, opinions and data contained in all publications are solely those of the individual author(s) and contributor(s) and not of MDPI and/or the editor(s). MDPI and/or the editor(s) disclaim responsibility for any injury to people or property resulting from any ideas, methods, instructions or products referred to in the content.